

Calculation, characterization, and application of the time shift function in wavelength-division-multiplexed return-to-zero systems

Oleg V. Sinkin, Vladimir S. Grigoryan, John Zweck, and Curtis R. Menyuk

University of Maryland Baltimore County, 1000 Hilltop Circle, Baltimore, Maryland 21250

Andrew Docherty and Mark Ablowitz

University of Colorado, Box 526, Boulder, Colorado 80309

Received January 3, 2005

We calculate the time shift function for collisions of pairs of pulses in different channels in a prototypical return-to-zero wavelength-division-multiplexed system with dispersion management and precompensation and postcompensation. Once the time shift function is known, the impairments that are due to collision-induced timing jitter can be rapidly determined. We characterize the shape of this function and determine how it scales with the initial pulse separation in time and with channel separation in wavelength. Finally, we apply it to the calculation of the worst-case time shift. © 2005 Optical Society of America

OCIS codes: 060.2330, 060.4370.

In wavelength-division multiplexed (WDM) return-to-zero (RZ) systems, collision-induced timing jitter is typically the major nonlinear effect that degrades the performance. Hence several methods have been developed to model timing jitter and reduce its effects.^{1–8} Much of this work is focused on solitons,^{1–4,6} but recent work has focused on quasi-linear systems as well.^{3,5,7,8} An important simplifying assumption in all theoretical work except complete simulations is that an optical pulse's total time shift is the sum of time shifts that are due to independent pairwise collisions. The validity of this assumption is not obvious because, in modern-day systems, optical pulses overlap many other pulses simultaneously owing to dispersion. Nonetheless, simulations demonstrate the validity of this assumption in both soliton and quasi-linear systems,³ and some of us recently showed that it produces a computation of the probability density function of the time shifts that is accurate over 10 orders of magnitude.⁷ This assumption vastly reduces the computer time that is required for calculating the distribution of time shifts and the impairments induced in WDM RZ systems.^{3,7} It also leads to important insights into the origin of timing jitter and to the development of ways to reduce it.^{4,6,8,9}

The analysis of collision-induced timing jitter and its effects begins with the calculation and characterization of the time shift function—the function that describes the time shift of an optical pulse in one WDM channel as a result of a pulse in another channel, as a function of the initial time separation between the pulses and the wavelength separation between the channels. Once this time shift function has been found, it can be used to calculate the distribution of impairments that are due to timing jitter,⁷ to design line codes,⁹ and for numerous other purposes. Earlier, some of us showed how to calculate this function by using an asymptotic analysis.^{5,10} With this analysis, it is possible to calculate the general shape

of this function in quasi-linear systems and to show that the function obeys a scaling law in which its duration increases as Δf , and its magnitude decreases as $(\Delta f)^{-2}$, where Δf is the frequency separation between the two WDM channels.^{5,10} In this Letter we calculate the time shift function in a quasi-linear system for a realistic dispersion map with precompensation and postcompensation that closely resemble what is found in undersea systems,⁷ using the computationally determined two-pulse interactions.³ We find that the scaling predicted by the asymptotic analysis in simpler systems^{5,10} holds approximately, but not exactly, and we discuss the physics of this function's behavior. We then apply this function to determine the worst-case bit patterns. Determining these patterns is important because the time shift distribution is approximately Gaussian up to approximately half of the cutoff times determined by these patterns.⁷

We refer to the pulse with respect to which we are calculating the time shift function as the target pulse and the channel in which it is located as the probe channel. The other WDM channels are referred to as the pump channels. We assume that the bit slots are initially aligned in all the WDM channels and number the bit slots from the bit slot of the target pulse such that the target pulse occupies bit slot 0. We write the time shift function as $\tau(\Delta f, l)$, where l is the initial offset of a bit slot in a pump channel that is separated by Δf from the probe channel. For a particular pattern of 1s and 0s the total time shift of the target pulse is

$$T_{\text{total}} = \sum_{k,l} \alpha_{kl} \tau(\Delta f, l), \quad (1)$$

where k indexes the pump channels and where $\alpha_{kl} = 1$ if the l th bit slot in the k th channel contains a pulse, corresponding to a digital 1, and is 0 otherwise. The time shift of target pulse u_T after propaga-

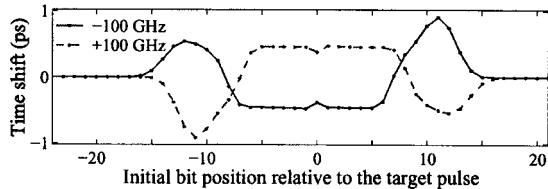


Fig. 1. Time shift function for two pump channels.

tion distance L as a result of a collision with a pulse u_{kl} in a pump channel is given by

$$\tau(\Delta f_k, l) = \frac{\lambda^2}{2\pi c} \int_0^L \Delta\Omega_{kl}(z) D(z) dz, \quad (2)$$

where $D(z)$ is the dispersion parameter ps/nm/km and $\Delta\Omega_{kl}(z)$ is the collision-induced frequency shift, given by

$$\frac{d\Delta\Omega_{kl}}{dz} = \frac{2\gamma}{E_T(z)} \int_{-\infty}^{\infty} |u_T(z, t)|^2 \frac{\partial |u_{kl}(z, t)|^2}{\partial t} dt, \quad (3)$$

where $E_T(z)$ is the target pulse energy and γ is the Kerr coefficient. This calculation takes into account gain and loss as well as the nonlinear interactions and dispersion.³

We consider a 10 Gbit/s system with a propagation distance of approximately 5000 km.⁷ The transmission part included 100 periods of the dispersion map consisting of 34 km of D_+ fiber and 17.44 km of D_- fiber followed by an amplifier. The values of dispersion, effective core area, nonlinear index, and loss were, respectively, 20.17 ps/(nm/km), 106.7 μm^2 , $1.7 \times 10^{-20} \text{ m}^2/\text{W}$, and 0.19 dB/km for the D_+ fiber and -40.8 ps/(nm/km), 31.1 μm^2 , $2.2 \times 10^{-20} \text{ m}^2/\text{W}$, and 0.25 dB/km for the D_- fiber. The average map dispersion is -0.5 ps/(nm/km), and the amount of precompensation and postcompensation is 1028 and 1815 ps/nm, respectively, which we optimized by minimizing the interchannel nonlinear amplitude distortion. We used 35 ps raised-cosine pulses with a peak power of 5 mW; the channels were copolarized. We did not consider noise.

In Fig. 1, we plot the time shift function, using Eq. (2), for the two pump channels with $\Delta f = \pm 100$ GHz. We note first that $\tau(\Delta f, l) = -\tau(-\Delta f, -l)$. This symmetry is exact if there is no higher-order dispersion, as was reported previously for soliton systems.⁴ We also observe that, as l increases from $-\infty$ in the pump channel with $\Delta f = -100$ GHz, the time shift starts from zero, becomes positive, then changes sign in the neighborhood of $l = -8$, becoming negative, after which it becomes positive again, and finally decays to zero. We have observed this behavior in a variety of systems, and it appears to be generic. We now explain its physical origin.

In long-haul systems with dispersion management, two pulses in different WDM channels move rapidly back and forth with respect to each other, resulting in multiple collisions, each of which we refer to as a microcollision. If, as is typically the case, the average map dispersion is nonzero, two pulses gradually pass

through each other while they experience multiple microcollisions. We refer to this process as a macrocollision. Consider now the collision dynamics of the target pulse with pulses in the pump channel with $\Delta f = -100$ GHz. Figure 2(a) shows the central times for the pulses with $l = 1, 11, -11$. The evolution of the frequency and time shifts of the target pulses owing to collisions with these three pulses is shown in Figs. 2(b) and 2(c). The pulse with $l = 1$ undergoes a complete macrocollision, while the pulses with $l = -11, 11$, undergo incomplete macrocollisions that occur at the beginning and the end of the system, respectively.

First we consider a complete macrocollision, as in $l = 1$. In its initial phase, the two interacting pulses undergo incomplete microcollisions. As the central time of the pump pulse relative to the target pulse is positive, from Eq. (3) the frequency shift after each incomplete microcollision increases. In the second phase of the macrocollision, the pulses undergo complete microcollisions with no significant change in the frequency shift. Finally, the pulses undergo incomplete microcollisions again, but now the frequency shift decreases, and it is nearly zero when the macrocollision is over. As the frequency shift is positive during most of the macrocollision and because the dispersion accumulated during the macrocollision is negative, the resultant time shift is negative, from Eq. (2). We note that the precompensation and postcompensation fibers have almost no effect on the time shift in a complete macrocollision. We next consider an incomplete macrocollision at the end of the system, as in $l = 11$. The frequency shift is positive because the pulses interact only during the initial phase of a macrocollision. The dispersion accumu-

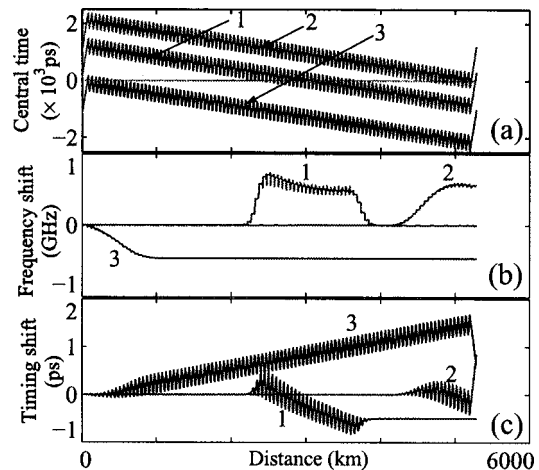


Fig. 2. Collision dynamics for three pulses.

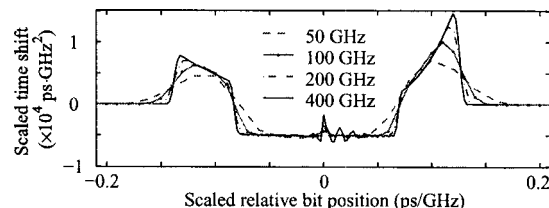


Fig. 3. Scaled time shift function.

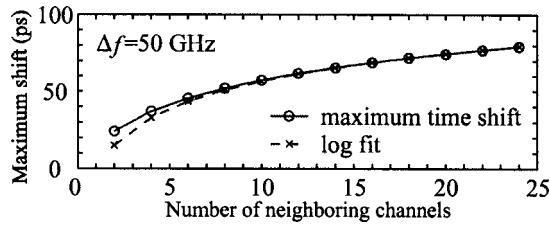


Fig. 4. Worst-case time shift versus number of channels.

lated during the macrocollision, including the post-compensation, is positive. Hence the time shift is positive. Finally, for an incomplete macrocollision at the start of the system, as in $l = -11$, the frequency shift is negative because the pulses interact only during the final phase of a complete macrocollision. After pulses have separated, the frequency shift is constant and negative. As the dispersion accumulated from the end of the collision to the end of the system is negative, the resultant timing shift is positive.

We found that the details of the dispersion map and transmission distance do not qualitatively affect the shape of $\tau(\Delta f, l)$ as long as the average map dispersion is large such that the length of the macrocollision is shorter than the system length, as is usually the case in realistic RZ systems. When the system length is larger than the collision length, we can still observe a similar behavior. However, in this case the details of the map can significantly affect the shape of $\tau(\Delta f, l)$.⁵ We note that a large average dispersion reduces the effects of nonlinearity, so the parameter regime considered here is more important in practice.

We now discuss how the time shift function scales. An asymptotic analysis^{5,10} predicts that $\tau(\Delta f, l) = a^2 \tau(a\Delta f, al)$, where a is a scaling parameter. In Fig. 3 we show $\tau(\Delta f, l)$ for channel spacings in the range $\Delta f = 50 - 400$ GHz. We have scaled τ by $(\Delta f)^2$ and l by $(\Delta f)^{-1}$. The scaling relation holds approximately, but there are significant deviations. From a physical standpoint, the scaling with the offset l occurs because the velocity difference between a pulse in a pump channel and the target pulse is proportional to Δf . In the scaling for τ , the time shift is determined mainly by the accumulation of residual frequency shifts that are due to incomplete microcollisions, as shown in Fig. 2, while the residual time shift is small. The frequency shift due to each microcollision is determined by the maximum overlap of pulses [Eq. (3)], which is independent of Δf , and the interaction length, which is proportional to $(\Delta f)^{-1}$. Hence the frequency shift that is due to each microcollision scales as $(\Delta f)^{-1}$. Because the number of incomplete microcollisions is proportional to $(\Delta f)^{-1}$, the total time shift scales as $(\Delta f)^{-2}$. For this scaling to hold, the number of incomplete microcollisions in each macrocollision should be large, and the maximum separation of the two pulses in each microcollision should be large compared with the pulse duration. When Δf is large, the first condition is violated, and oscillations are visible when $\Delta f = 400$ GHz. When Δf is small, the second condition is violated, blurring the distinction between complete and incomplete macrocollisions, so the tran-

sition between the two occurs more gradually, as can be seen when $\Delta f = 50$ GHz.

Given $\tau(\Delta f, l)$, we determine the worst-case time shift from Eq. (1) by setting $\alpha_{kl} = 1$ when $\tau(\Delta f_k, l) > 0$ and $\alpha_{kl} = 0$ when $\tau(\Delta f_k, l) < 0$ or vice versa. From the relation $\tau(\Delta f, l) = -\tau(-\Delta f, -l)$, we find that the worst case corresponds to an opposite choice of 1s and 0s in channels with $\pm \Delta f$, just as Xu *et al.*⁴ discovered for solitons. From scaling relation $\tau(\Delta f, l) = a^2 \tau(a\Delta f, al)$, we would also conclude, with Xu *et al.*,⁴ that the maximum time shift increases logarithmically with the number of channels, as shown in Fig. 4, where we have fitted a logarithmic function of the form $a + b \log N$. This scaling relation breaks down when all microcollisions are complete, which corresponds to $N > 16$ for the system that we studied. However, the residual time shift that is due to microcollisions still scales as $(\Delta f)^{-2}$, because the frequency excursion is proportional to $(\Delta f)^{-1}$ and so is the length of the microcollision. Hence, as shown in Fig. 4, the maximum time shift continues to increase logarithmically beyond $N = 16$.

In conclusion, we have discussed the importance of the time shift function and calculated it for a prototypical quasi-linear WDM-RZ system with precompensation and postcompensation. We described the physical origin of its characteristic shape, which we have observed in a variety of systems. We also discussed its scaling properties and the limits in which this scaling holds. Finally, we applied the time shift function to the calculation of the worst-case time shift.

O. V. Sinkin's e-mail address is osinkil@umbc.edu.

References

1. H. Sagahara, A. Maruta, and Y. Kodama, *Opt. Lett.* **24**, 145 (1999).
2. P. V. Mamyshev and L. Mollenauer, *Opt. Lett.* **24**, 448 (1999).
3. V. S. Grigoryan and A. Richter, *J. Lightwave Technol.* **18**, 1148 (2000).
4. C. Xu, C. Xie, and L. Mollenauer, *Opt. Lett.* **27**, 1303 (2002).
5. M. J. Ablowitz, A. Docherty, and T. Hirooka, *Opt. Lett.* **28**, 1191 (2003), and references therein.
6. X. Liu, X. Wei, L. F. Mollenauer, C. J. McKinstrie, and C. Xie, *Opt. Lett.* **28**, 1412 (2003), and references therein.
7. O. V. Sinkin, V. S. Grigoryan, R. Holzlohner, A. Kalra, J. Zweck, and C. R. Menyuk, in *Optical Fiber Communication Conference (OFC)*, Vol. 95 of OSA Trends in Optics and Photonics Series (Optical Society of America, 2004), paper TUN4.
8. M. J. Ablowitz, C. Ahrens, G. Biondini, S. Chakravarty, and A. Docherty, *Opt. Lett.* **29**, 2354 (2004).
9. W. Wang, O. V. Sinkin, T. Adali, J. Zweck, and C. R. Menyuk, in *Conference on Lasers and Electro-Optics (CLEO)*, Vol. 96 of OSA Trends in Optics and Photonics Series (Optical Society of America, 2004), paper CFN5.
10. A. Docherty, "Collision induced timing shifts in wavelength-division-multiplexed optical fiber communication systems," Ph.D. dissertation (University of New South Wales, Sydney, Australia, 2004).